DMD Fast Forward. Published on June 10, 2019 as DOI: 10.1124/dmd.119.087015
This article has not been copyedited and formatted. The final version may differ from this version.

Role of Molybdenum-Containing Enzymes in the Biotransformation of the Novel Ghrelin Receptor Inverse Agonist PF-5190457: A Reverse Translational Bed-to-Bench Approach

Sravani Adusumalli[1], Rohitash Jamwal[1], R. Scott Obach[2], Tim F. Ryder[2], Lorenzo Leggio[3,4,5], Fatemeh Akhlaghi[1*]

1. Clinical Pharmacokinetics Research Laboratory, Department of Biomedical and Pharmaceutical Sciences, University of Rhode Island Kingston, RI, USA
2. Department of Pharmacokinetics, Dynamics, and Metabolism, Pfizer, Inc., Groton, CT, USA
3. Section on Clinical Psychoneuroendocrinology and Neuropsychopharmacology, National Institute on Alcohol Abuse and Alcoholism Division of Intramural Clinical and Biological Research and National Institute on Drug Abuse Intramural Research Program, Bethesda, MD, USA
4. Medication Development Program, National Institute on Drug Abuse Intramural Research Program, Baltimore, MD, USA
5. Center for Alcohol and Addiction Studies, Department of Behavioral and Social Sciences, Brown University, Providence, RI, USA

Downloaded from dmd.aspetjournals.org at ASPET Journals on April 18, 2024

DMD Fast Forward. Published on June 10, 2019 as DOI: 10.1124/dmd.119.087015
This article has not been copyedited and formatted. The final version may differ from this version.

Running title: Biotransformation of PF-5190457

***Corresponding author:**

Fatemeh Akhlaghi

Clinical Pharmacokinetics Research Laboratory,

Department of Biomedical and Pharmaceutical Sciences,

Avedisian Hall, 7 Greenhouse Road,

University of Rhode Island, Kingston, RI, USA

fatemeh@uri.edu

Count:

Number of text pages - 16

Number of figures – 7

Number of tables - 1

Number of references - 50

Number of words in Abstract - 243

Number of words in Introduction - 590

Number of words in Discussion - 1023

Nonstandard abbreviations:

ABT- 1 amino benzotriazole; AO - Aldehyde oxidase; AUD - Alcohol use disorder; GHS-R1a - Growth hormone secretagogue receptor 1a; HMBC - Heteronuclear multiple bond correlation; HSQC - Heteronuclear single quantum coherence; HLC - Human liver cytosol; HLM - Human liver microsomes; IS - Internal standard; rAOX - Recombinant aldehyde oxidase; XO - Xanthine oxidase

Downloaded from dmd.aspetjournals.org at ASPET Journals on April 18, 2024

DMD Fast Forward. Published on June 10, 2019 as DOI: 10.1124/dmd.119.087015
This article has not been copyedited and formatted. The final version may differ from this version.

Abstract

PF-5190457 ((R)-2-(2-methylimidazo[2,1-b]thiazol-6-yl)-1-(2-(5-(6-methylpyrimidin-4-yl)-2,3-dihydro-1H-inden-1-yl)-2,7-diazaspiro[3.5]nonan-7-yl)ethan-1-one) was identified as a potent and selective inverse agonist of the ghrelin receptor (GHS-R1a). The present translational bed-to-bench work characterizes the biotransformation of this compound *in vivo* and then further explores *in vitro* metabolism in fractions of human liver and primary hepatocytes. Following oral administration of PF-5190457 in a Phase 1b clinical study, hydroxyl metabolites of the compound were observed, including one that had not been observed in previously performed human liver microsomal incubations. PF-6870961 was biosynthesized using liver cytosol, and the site of hydroxylation was shown to be on the pyrimidine using nuclear magnetic resonance spectroscopy. The aldehyde oxidase (AO) inhibitor raloxifene and the xanthine oxidase (XO) inhibitor febuxostat inhibited the formation of PF-6870961 in human liver cytosol, suggesting both enzymes were involved in the metabolism of the drug. However, greater inhibition was observed with raloxifene, indicating AO to be a dominant enzyme in the biotransformation. The intrinsic clearance of the drug in human liver cytosol was estimated to be 0.002 mL/min/mg protein. This study provides important novel information at three levels: 1) it provides additional new information on the recently developed novel compound PF-5190457, the first GHS-R1a blocker that has moved to development in humans; 2) it provides an example of a reverse translational approach where a discovery in humans was brought back, validated and further investigated at the bench level; and 3) it demonstrates the importance of considering the molybdenum-containing oxidases during the development of new drug entities.

Downloaded from dmd.aspetjournals.org at ASPET Journals on April 18, 2024

DMD Fast Forward. Published on June 10, 2019 as DOI: 10.1124/dmd.119.087015
This article has not been copyedited and formatted. The final version may differ from this version.

Significance statement: PF-5190457 is a novel ghrelin receptor inverse agonist that is currently undergoing clinical development for treatment of alcohol use disorder. PF-6870961**,** a major hydroxyl metabolite of the compound, were observed in human plasma, but was absent in human liver microsomal incubations. PF-6870961 was biosynthesized using liver cytosol, and the site of hydroxylation on the pyrimidine ring was characterized. Inhibitors of aldehyde oxidase (AO) and xanthine oxidase (XO) inhibited the formation of PF-6870961 in human liver cytosol, suggesting both enzymes were involved in the metabolism of the drug. This information is important for patient selection for subsequent clinical studies.

Downloaded from dmd.aspetjournals.org at ASPET Journals on April 18, 2024

DMD Fast Forward. Published on June 10, 2019 as DOI: 10.1124/dmd.119.087015
This article has not been copyedited and formatted. The final version may differ from this version.

Introduction

Ghrelin is a 28-amino acid peptide produced by endocrine cells primarily localized in the stomach. Ghrelin plays key roles in growth, appetite, food intake, glucose homeostasis, metabolism and energy balance (Kojima et al., 1999; Asakawa et al., 2001; Inui et al., 2004; Nagaya et al., 2004; Neary et al., 2004; Nagaya et al., 2005; Tong et al., 2010). In its acylated form (acyl-ghrelin, traditionally referred to as "active ghrelin"), ghrelin binds to and activates the main ghrelin receptor named growth hormone secretagogue receptor 1a (GHS-R1a), a G protein-coupled receptor with high intrinsic activity (Howard et al., 1996; Damian et al., 2012).

Recent research has focused on the overlap between obesity and addictions and how neurotransmitters and peptides regulating food intake can also influence craving for alcohol in alcohol-dependent individuals (Leggio et al., 2011; Volkow et al., 2013). Among others, the ghrelin system has been investigated in animal models and patients with alcohol-dependence, and collectively these studies support a role of ghrelin in alcohol-seeking behaviors. Specifically, several rodent studies support the notion that the ghrelin system is causally involved in alcohol-seeking behaviors and these data have been further corroborated by human studies indicating an association between alcohol craving and drinking and the subjective effects of alcohol with the endogenous concentrations of peripheral ghrelin (Leggio, 2010; Zallar et al., 2017; Morris et al., 2018). Furthermore, two double-blind placebo-controlled human laboratory studies, have shown that, intravenous administration of ghrelin in alcohol-dependent heavy drinkers leads to increased cue-induced alcohol craving in a bar-like setting (Leggio et al., 2014) and to increased alcohol self-administration and modulation of brain activity in areas involved in alcohol-seeking behaviors (Farokhnia et al., 2018). Together, rodent and human studies collectively suggest that blockade of GHS-R1a may represent a potentially novel pharmacological approach to treat alcohol use disorder (AUD).

PF-5190457 ((R)-2-(2-methylimidazo[2,1-b]thiazol-6-yl)-1-(2-(5-(6-methylpyrimidin-4-yl)-2,3-dihydro-1H-inden-1-yl)-2,7-diazaspiro[3.5]nonan-7-yl)ethan-1-one) is a member of a spiro-azetidino-

Downloaded from dmd.aspetjournals.org at ASPET Journals on April 18, 2024

DMD Fast Forward. Published on June 10, 2019 as DOI: 10.1124/dmd.119.087015
This article has not been copyedited and formatted. The final version may differ from this version.

piperidine series identified as a potent ghrelin receptor inverse agonist (Bhattacharya et al., 2014). PF-5190457 represents the first ghrelin receptor blocker that moved to clinical development and a recent Phase 1b drug-alcohol interaction placebo-controlled study showed the safety and tolerability of PF-5190457 when administered to heavy drinkers, including its co-administration together with an oral alcohol challenge (Lee et al., 2018). As an additional safety outcome, this Phase 1b study showed that PF-5190457 did not affect alcohol pharmacokinetics and it also showed indirectly that alcohol does not affect the pharmacokinetics of PF-5190457.

Limited information is available on the biotransformation of PF-5190457. The assessment of metabolic pathways of a new drug is important as it helps to understand the pharmacokinetics and pharmacodynamics of the compound in humans. It is also essential to identify the enzymes responsible for biotransformation, as this information contributes to an understanding of interindividual variability in pharmacokinetics that can be due to genetic polymorphism and/or drug-drug interactions. Additionally, metabolites generated by these enzymes could be pharmacologically active on the same receptor as the parent compound and/or have off-target effects (Lin and Lu, 1997; Kumar and Surapaneni, 2001; Fu et al., 2013).

The present study describes the biotransformation of PF-5190457 *in vitro* and the identification of PF-6870961 in humans. Specifically, the objectives of the present study were: 1) characterization of the circulating metabolites *in vivo* in human plasma, 2) determination of formation of metabolites *in vitro*, in sub-cellular fractions of human liver and human hepatocytes, 3) determination of the structure of metabolites by mass spectrometry and NMR analyses, 4) assessment of the kinetic parameters of metabolite formation, and 5) identification of the enzyme/s responsible for the formation of PF-6870961 using specific inhibitors for each enzyme.

Downloaded from dmd.aspetjournals.org at ASPET Journals on April 18, 2024

DMD Fast Forward. Published on June 10, 2019 as DOI: 10.1124/dmd.119.087015
This article has not been copyedited and formatted. The final version may differ from this version.

Materials and Methods

PF-5190457, raloxifene hydrochloride, febuxostat, and tacrine were procured from Sigma Aldrich (St. Louise, MO, USA). Allopurinol was purchased from Toronto Research Chemicals (Toronto, Canada). Major circulating hydroxy metabolite of PF-5190457 (also called PF-6870961) was biosynthesized as described below. Recombinant aldehyde oxidase (rAOX) was produced by Dr. Ciaran Cronin, Pfizer, La Jolla, CA, USA. NADPH tetrasodium salt was obtained from Calbiochem (EMD Millipore, Billerica, MA). LC-MS grade methanol, acetonitrile, and formic acid were from Fisher Scientific (Fairlawn, NJ, USA). All other reagents and chemicals used in the study were of analytical grade and used without further purification.

In Vivo Metabolite Profiling

Sample preparation

Plasma samples from a recent Phase 1b study were analyzed by high-resolution mass spectrometry (HRMS) to identify the circulating metabolites (Lee et al., 2018). Plasma samples from 100 mg b.i.d. dose (patient ID N101, N102, N103) were pooled and prepared for metabolite profiling experiments at various sampling times [predose, early (30 and 60 min), late (1350 and 1440 min)]. Plasma proteins were precipitated with the addition of acetonitrile (5 mL) followed by vortex mixing and centrifugation at 1,700 *g* for 5 min. The supernatant was transferred and evaporated for 4 h in a vacuum centrifuge (Genevac, SP Scientific, Gardiner, NY), and subsequently reconstituted in 30 µL acetonitrile followed by addition of 120 µL water. The reconstituted samples were spun for 3 min to remove particulates, and 10 µL of an aliquot of the reconstituted solution was injected onto a UHPLC-HRMS system.

High-Resolution mass spectrometry

Chromatographic separation for metabolite profiling was achieved using a Waters HSS-T3 C18 column (1.8 µm; 2.1×100 mm; Waters Corp., Milford, MA) maintained at 45°C in line with a Thermo Accela

Downloaded from dmd.aspetjournals.org at ASPET Journals on April 18, 2024

DMD Fast Forward. Published on June 10, 2019 as DOI: 10.1124/dmd.119.087015
This article has not been copyedited and formatted. The final version may differ from this version.

HPLC pump, CTC Analytics autoinjector, a photodiode array detector and a Thermo Orbitrap Elite ion trap high-resolution mass spectrometer (HRMS) (Thermo Fisher Scientific Inc, Waltham, MA, USA). The mobile phase consisted of 10 mM ammonium acetate (A) and acetonitrile (B), and separation was achieved at a flow rate of 0.35 mL/min. The gradient elution was started from 5% B, maintained for 0.5 min, increased to 50% B over 10 min, and then to 95% B over the next 2 min and finally decreased to 5% B to re-equilibrate the column with a total run time of 15 min. The MS detector was operated in positive ion electrospray (ESI +) mode.

In Vitro Biotransformation of PF-5190457

Preparation of subcellular fractions

Human liver tissues and human hepatocytes were obtained from Xenotech (Lenexa, KS, USA). The hepatocytes, liver microsomes or cytosols were pooled from donors of both sexes. Human liver microsomal (HLM) and cytosolic (HLC) fractions were prepared by differential ultracentrifugation from the human liver as described previously (Jamwal et al., 2017). Total protein concentration for the HLM and HLC were determined using Pierce BCA (bicinchoninic acid) protein assay kit (Thermo Fisher Scientific Inc, Waltham, MA, USA) and the fractions were stored in -80°C until further analysis.

HLM and HLC incubations

The *in vitro* metabolism of PF-5190457 was studied using HLM and HLC fractions. PF-5190457 was incubated (50-100 μM) with pooled HLM and HLC in 100 mM potassium phosphate buffer (pH 7.4), and methanol concentration from substrate addition was kept below 0.5%. Incubations were conducted at 37°C in a water bath, and the total incubation mixture volume was 50 μL. The total protein concentration used for both HLM and HLC ranged from 0.05 - 2 mg/mL. PF-5190457 was also incubated in only 100 mM potassium phosphate buffer (pH 7.4) without HLM or HLC as a control. Microsomal incubations were conducted with and without the addition of NADPH. Reactions in HLM and HLC were initiated by the addition of substrate. The reaction was terminated by the addition of 200 μL of ice-cold methanol at

Downloaded from dmd.aspetjournals.org at ASPET Journals on April 18, 2024

DMD Fast Forward. Published on June 10, 2019 as DOI: 10.1124/dmd.119.087015
This article has not been copyedited and formatted. The final version may differ from this version.

various incubation times (0-120 min). Subsequently, the samples were centrifuged for 5 min at 10,000 rpm to remove the precipitated protein and were analyzed as described below.

LC-MS/MS analysis of HLM and HLC samples

Samples were analyzed using an Acquity UPLC coupled with a Xevo-TQ mass spectrometer (Waters Corp, Milford, MA, USA). Analytes were chromatographically separated on a C18 column (Acquity UPLC BEH 2.1×50 mm) with 1.7 µm particle size and 130 Å porosity. A pre-column (Acquity UPLC BEH C18, 2.1×5 mm) was connected prior to the analytical column. Mobile phase consisted of water:methanol (95:5, v/v) containing 0.1% formic acid (A) and 100% methanol containing 0.1% formic acid (B). The column and autosampler temperature were kept at 40 and 10°C, respectively. The mobile phase was delivered at a flow rate of 0.25 mL/min, and the injection volume was 5 µL. The total assay run time was 12.30 min. Mobile phase A was maintained at 98% for initial 2 min, decreased to 50% at 8.30 min and to 5% over the next 2 min and then returned to the initial conditions for equilibration at 10.30 min. A full scan from 100-1200 Da was carried out in a positive electrospray ionization mode with the following parameters: desolvation temperature - 600°C, desolvation gas flow - 1000 L/h, capillary voltage - 3.50 kV and cone voltage - 30 V. Similarly, single-ion monitoring for the $[M+H]^+$ ions of the PF-5190457 (*m/z* 513.2) and anticipated metabolites, i.e., hydroxy metabolite (*m/z* 513.2+16), glucuronide (*m/z* 513.2+176) and hydroxy glucuronide (*m/z* 513.2+192) was performed (table 1).

Hepatocytes incubations

PF-05190457 was incubated in pooled cryopreserved human hepatocytes (750000 cells/mL; In Vitro Technologies, Baltimore, MD) with and without 1 amino benzotriazole (ABT), a pan CYP450 inhibitor, at 1 mM or hydralazine, a selective probe inactivator of aldehyde oxidase (AO) at 0.05 mM (Ortiz de Montellano and Mathews, 1981; Strelevitz et al., 2012). Incubations were carried out on a rotating shaker placed in an incubator maintained under an atmosphere of O_2/CO_2 (95:5) and relative humidity of 75%.

Downloaded from dmd.aspetjournals.org at ASPET Journals on April 18, 2024

DMD Fast Forward. Published on June 10, 2019 as DOI: 10.1124/dmd.119.087015
This article has not been copyedited and formatted. The final version may differ from this version.

Incubations were carried out for 4 h and were stopped by snap-freezing in a dry ice-acetone bath. Samples were prepared and analyzed as described above for HLM and HLC incubations.

Biosynthesis and NMR Analysis

Biosynthesis of PF-6870961, the major hydroxy metabolite of PF-5190457

PF-5190457 (20 µM) was incubated with female mouse liver cytosol (2.0 mg/mL; Corning-Gentest, Woburn, MA) in 40 mL potassium phosphate buffer (100 mM, pH 7.5) in a shaking water bath maintained at 37°C for 1.5 hr. The incubation was terminated with the addition of CH_3CN (40 mL), and the precipitated material was removed by spinning in a centrifuge for 5 min at 1,700 g. The supernatant was partially evaporated in a Genevac vacuum centrifuge for 2 hr. To the remaining mixture was added 0.25 mL neat formic acid, 0.25 mL CH_3CN, and water to a final volume of 25 mL. This mixture was spun in a centrifuge at 40,000 g for 30 min and clarified supernatant was applied to an HPLC column (Polaris C18, 4.6×250 mm; 5 µm) through a Jasco HPLC pump at a rate of 0.8 mL/min. After the entire sample was applied, an additional ~5 mL of mobile phase (0.1% formic acid containing 1% CH_3CN) was pumped through the system. The column was moved to a Thermo LTQ HPLC-MS system containing a photodiode array detector, and a mobile phase gradient was applied to elute material of interest. The mobile phase was comprised of 0.1% formic acid in water (A) and CH_3CN (B) and was run at a flow rate of 0.8 mL/min. The gradient began at a composition of 2%B for 5 min followed by a linear gradient to 25%B at 70 min. The eluent passed through the photodiode array detector scanning from 200-400 nm and then to a splitter (ratio was approximately 15:1) with the larger portion going to a CTC Leaptec fraction collector (CTC, Cary, NC). Fractions were collected every 20 sec. The remainder was introduced into the mass spectrometer operated in the positive ion mode. The fractions proposed to contain the hydroxy metabolites of interest were analyzed for identity and purity on a Thermo Orbitrap Elite UHPLC-UV-MS system containing an Acquity column (HSS T3 C18, 2.1×100 mm, 1.7 µm particle size) using the method described above at a flow rate of 0.4 mL/min and an injection volume of 5 µL. Fractions

Downloaded from dmd.aspetjournals.org at ASPET Journals on April 18, 2024

DMD Fast Forward. Published on June 10, 2019 as DOI: 10.1124/dmd.119.087015
This article has not been copyedited and formatted. The final version may differ from this version.

containing single peaks by UV and the desired protonated molecular ions were combined and evaporated by vacuum centrifugation for analysis by NMR spectroscopy. Samples were reconstituted with 100 µL of DMSO-d6 "100%" (Cambridge Isotope Laboratories, Andover, MA) before NMR analysis and ^{1}H, and 2D NMR (^{1}H COSY, HMBC, and HSQC) analyses were carried out as described below.

NMR Sample Analysis

Isolated samples were reconstituted in 0.10 mL of DMSO-d6 "100%" and placed in a 1.7 mm NMR tube which had been stored in a dry argon atmosphere. The ^{1}H and ^{13}C spectra were referenced using residual DMSO-d6 (^{1}H δ=2.50 ppm relative to TMS, δ=0.00, ^{13}C δ=39.50 ppm relative to TMS, δ=0.00). NMR spectra were recorded on a Bruker Avance 600 MHz (Bruker BioSpin Corporation, Billerica, MA) controlled by Topspin V3.2 and equipped with a 1.7 mm TCI Cryo probe. 1D spectra were recorded using an approximate sweep width of 8400 Hz, and a total recycle time of approximately 7 s. The resulting time-averaged free induction decays were transformed using an exponential line broadening of 1.0 Hz to enhance the signal to noise. The 2D data were recorded using the standard pulse sequences provided by Bruker. At a minimum, a 1K x 128 data matrix was acquired using a minimum of 2 scans and 16 dummy scans with a spectral width of 10000 Hz in the f2 dimension. The 2D data sets were zero-filled to at least 1k data point. Post-acquisition data processing was performed with Topspin V3.2 MestReNova. Quantitation of NMR isolates was performed by external calibration against the 1H NMR spectrum of 5 mM benzoic acid standard compared to that of the isolated metabolites using the ERETIC2 function within Topspin V3.2

Enzyme Kinetic Studies

The formation of the PF-6870961 in rAOX and HLC fraction was studied to determine the enzyme kinetic parameters. Before the assessment of the enzyme kinetics, protein concentration and incubation time linearity of PF-6870961 formation were evaluated to choose optimum conditions.

Downloaded from dmd.aspetjournals.org at ASPET Journals on April 18, 2024

DMD Fast Forward. Published on June 10, 2019 as DOI: 10.1124/dmd.119.087015
This article has not been copyedited and formatted. The final version may differ from this version.

rAOX incubations

PF-5190457 (0.5-125 µM) was incubated with rAOX (0.090 mg/mL) in 100 mM potassium phosphate buffer. The incubations were conducted at 37 °C in shaking water bath. The incubation mixture volume was 50 µL, and all incubations were performed in triplicate. The reactions were terminated after 120 min using methanol containing 2.5 ng/mL tacrine (internal standard). Samples were processed and analyzed as described below.

HLC incubations

Kinetic parameters for the formation of PF-6870961 from PF-5190457 was determined by incubating the drug in pooled, allopurinol/oxypurinol free, HLC (**Supplemental Information I**). The optimized total protein concentration and incubation times in HLC were 0.1 mg/mL and 5 min, respectively. PF-5190457 (0.05–100 µM) with HLC in a total volume of 50 µL of 100 mM potassium phosphate buffer (pH-7.4) were incubated at 37°C in duplicate. The final concentration of methanol in the incubations was <0.25%. The reaction was initiated by the addition of cytosol and terminated by protein precipitation with the addition of methanol (200 µl) containing the 2.5 ng/mL tacrine as IS.

LC-MS/MS analysis for kinetic studies

All the samples from rAOX and HLC incubations were centrifuged for 5 min at 10,000 *rpm*. The supernatants were removed and analyzed as follows. The parent, metabolite, and IS were monitored using Xevo TQ-MS (Waters Corp., Milford, MA, USA) coupled to Acquity UPLC system (Waters Corp., Milford, MA, USA). The analytes were separated using an Aquity UPLC BEH C18 (2.1 x 50 mm, 1.7 µm particle size, 130Ǻ pore size) analytical column with an Acquity UPLC BEH C18 VanGuard pre-column (2.1 x 5 mm, 130Ǻ). Mobile phase solution A consisted of water: methanol 95/5 % (v/v) and mobile phase solution B consisted of methanol (100%). Formic acid (0.1%) was added to both the mobile phase solutions. The flow rate was 0.25 mL/min with a 10.30 min run-time. The column temperature was maintained at 40 °C. The gradient consisted of 2% methanol for 2 min, increased to 35% for 2.0 - 7.30

Downloaded from dmd.aspetjournals.org at ASPET Journals on April 18, 2024

DMD Fast Forward. Published on June 10, 2019 as DOI: 10.1124/dmd.119.087015
This article has not been copyedited and formatted. The final version may differ from this version.

min, further increased to 95% methanol at 8 min and held until 8.30 min before returning to initial conditions to equilibrate with a total run time of 10.30 min. Mass spectral analysis and quantification were carried out using MRM on a positive electrospray ionization mode with the following parameters: desolvation temperature of 350 °C, desolvation gas flow 650 L/h, capillary voltage 3.50 kV and cone voltage 20 V. The optimized settings of mass spectrometer voltage and the retention time (R_t) for the analytes and IS with quantifier and qualifier fragments are summarized in **Supplemental Table 1**. Data acquisition and processing were performed using MassLynx™ (V 4.1) and TargetLynx™, respectively. Retention times for PF-6870961 and internal standards were 4.4 and 5.1 min, respectively. Quantitation was done using PF-6870961 standard curve ranging from 0.1-1 µM. The calibration standards were within ± 15% of nominal values.

Inhibition Studies

Incubation of PF-5190457 in HLC (with AO and XO inhibitors)

PF-5190457 (25 µM) was incubated with pooled allopurinol/oxypurinol free HLC (0.1 mg/ml, n=9) in a total volume of 50 µL of 100 mM potassium phosphate buffer (pH 7.4) in the presence and absence of inhibitors. Incubation conditions were similar to previous HLC kinetic experiments. To identify the enzymes involved in the formation of PF-6870961, HLC was incubated with and without AO inhibitor (raloxifene 0.005-50 µM), and XO inhibitor (febuxostat 0.001-50 µM). The reactions were terminated at 5 min using methanol containing 2.5 ng/mL tacrine (IS). The samples were analyzed using LC-MS/MS as described under enzyme kinetic studies.

Data Analysis

Estimations of the maximum rate of PF-6870961 formation (V_{max}) and the Michaelis-Menten constant (K_m) were performed using nonlinear-regression analysis within Prism 6 (GraphPad Software Inc., La Jolla, CA) using the Michaelis-Menten equation [$V = (V_{max}*S)/(K_m+S)$].

The apparent *in vitro* intrinsic clearance (Cl_{int}) was calculated as V_{max}/K_m.

Downloaded from dmd.aspetjournals.org at ASPET Journals on April 18, 2024

DMD Fast Forward. Published on June 10, 2019 as DOI: 10.1124/dmd.119.087015
This article has not been copyedited and formatted. The final version may differ from this version.

Results

Characterization of PF-5190457 Metabolites in Human Plasma

The circulating metabolites of PF-5190457 were determined in the plasma of human subjects who were administered PF-5190457 orally in the Phase 1b clinical study (Lee et al., 2018) (**Fig. 1**). Two peaks with protonated molecular ions of 16 mass units greater than PF-5190457 were observed (*m/z* 529.2382), indicating the addition of oxygen. Fragment ions of PF-6870961 that had a greater ion abundance included *m/z* 351.2179, 305.1430, and 225.1022 is indicative of oxidative biotransformation on the indenyl-pyrimidine portion of the parent molecule. Additional metabolites proposed as glucuronide and hydroxy glucuronide conjugates (*m/z* 689 and 705) were detected at apparent lower levels in the plasma. A small signal peak in the mass spectrometer was observed indicating an addition of water (*m/z 531*), but no further information was obtained.

In Vitro Biotransformation of PF-5190457

HLM and HLC incubations

Experiments conducted in the subcellular fractions of human liver generated the PF-6870961 in HLC without the addition of cofactors (**Fig. 2a**). This metabolite was not observed in HLM supplemented with NADPH. PF-6870961 was detected in HLC as the protonated molecular ion $[M + H]^+$ at *m/z* 529 and produced fragments at *m/z* 225 and 351(**Fig. 2b**). The metabolite formed in HLC increased with incubation time, the concentration of substrate, and concentration of cytosol.

Hepatocytes incubations

The formation of PF-6870961 was observed in human hepatocytes as shown in the chromatogram **(Fig. 3)**. The traces are extracted ion chromatograms of m/z 529.2376 (5 ppm tolerance) representing the protonated molecular ion of a hydroxylated metabolite. The addition of ABT, a broad-spectrum P450 inactivator, inhibited the formation of the apparent minor metabolites at R_t 4.12, 4.62, and 5.57 min and did not affect the metabolite eluting at R_t 3.98 min suggesting that CYP mediated metabolism for the

Downloaded from dmd.aspetjournals.org at ASPET Journals on April 18, 2024

DMD Fast Forward. Published on June 10, 2019 as DOI: 10.1124/dmd.119.087015
This article has not been copyedited and formatted. The final version may differ from this version.

minor metabolites and not the major circulating metabolite, PF-6870961. It was also observed that the addition of hydralazine inhibited the formation of the metabolite at R_t 3.97 min indicating that AO could be the primary enzyme involved in the biotransformation of PF-5190457 in human liver (**Supplemental fig. 1**).

Identification of Metabolite by NMR Spectroscopy

^{1}H and 2D NMR analysis of the parent compound PF-05190457 were performed for comparison against the spectra of the isolated metabolite. (Full interpretation and spectra are included with the **Supplemental Fig. 2-10**). Comparison of the parent and metabolite ^{1}H spectrum shows one less aromatic proton with significant chemical shifts occurring on the 4-methylpyrimidine moiety (**Fig. 4**). The methylene group on the 4-methylpyrimidine moiety was observed intact with an upfield chemical shift from δ 2.51 to δ 2.27. The HSQC (heteronuclear single quantum coherence) spectrum of the parent compound demonstrated the protons of the methyl group of the 4-methylpyrimidine moiety at δ 2.51 were long ranged coupled into a carbon having a chemical shift of δ 115.8 which was determined to have an attached proton at δ 7.95 from the HSQC spectrum. Similarly, the HMBC (heteronuclear multiple bond correlation) spectrum of the metabolite demonstrated the protons of the methyl group of the 4-methylpyrimidine moiety at δ 2.27 were long ranged coupled into a carbon having a new chemical shift of δ 99.7 which was determined to have an attached proton at δ 6.86 from the HSQC spectrum. This suggests the proton ortho to the methyl group on the 4-methylpyrimidine moiety observed in the parent compound is still intact in the metabolite but shifted from δ 7.95 to δ 6.86. Also noted, in the ^{1}H spectrum of the metabolite, is the absence of the aromatic proton resonance at δ 9.05 observed in the parent compound. This was determined to be the proton meta to the methyl group on the 4-methylpyrimidine moiety between the two nitrogens. This suggests the site of oxidation is on the carbon between the two nitrogens of the 4-methylpyrimidine moiety.

Downloaded from dmd.aspetjournals.org at ASPET Journals on April 18, 2024

DMD Fast Forward. Published on June 10, 2019 as DOI: 10.1124/dmd.119.087015
This article has not been copyedited and formatted. The final version may differ from this version.

Enzyme Kinetic Analysis

Representative Michaelis-Menten kinetic plots of PF-6870961 formation in rAOX and HLC are depicted in **Fig. 5** and **Fig. 6**, respectively. Substrate inhibition kinetics at higher concentration of substrate was observed for rAOX incubations. The K_m and V_{max} values for the formation of PF-6870961 in rAOX and HLC were found to be 6.9±0.8 µM and 357.9±19.2 pmol/min/mg protein, and 42.8±4.1 µM and 119.6±3.6 pmol/min/mg protein, respectively. The CL_{int} in rAOX and HLC was 0.06 and 0.002 mL/min/mg protein, respectively. The differences in K_m values between HLC and rAOX are acknowledged but remain unexplained.

Biotransformation of PF-5190457 is mediated by AO and XO

The effect of AO (raloxifene) and XO (febuxostat) inhibitors on the metabolism of PF-5190457 in HLC was investigated. There was considerable (>75%) but not complete inhibition of formation of the PF-6870961 with 50 µM raloxifene **(Fig. 7).** The extent of inhibition with febuxostat was greater than 50% at 1 µM **(Fig. 7**), and a further increase in the inhibitor concentration did not reduce the formation of the metabolite. Thus, the maximum inhibition value in HLC is indicative of the maximum contribution of the affected enzyme. It can be concluded that both AO and XO contribute, and the inhibition values suggest that the contributions of each are of similar magnitude.

Downloaded from dmd.aspetjournals.org at ASPET Journals on April 18, 2024

DMD Fast Forward. Published on June 10, 2019 as DOI: 10.1124/dmd.119.087015
This article has not been copyedited and formatted. The final version may differ from this version.

Discussion

At present, AUD is the only potential target under study at least clinically for PF-5190457. Furthermore, Denney et al. suggest other indications (CNS indications like sleep problems, shift work disorder, Prader-Willi) rather than metabolic indications like diabetes [given the tachyphylaxis they saw after 14-day administration] (Denney et al., 2017). The characterization of circulating metabolites from patients orally administered with the ghrelin receptor inverse agonist PF-5190457 revealed the biotransformation pathways for this novel compound. The primary route of metabolism observed in humans was hydroxylation yielding PF-6870961**.** . In vitro experiments showed that this metabolite was generated in human liver cytosol. The metabolite observed as PF-6870961 (*m/z* 529a) in human plasma and the metabolite formed in HLC (*m/z* 529) showed a similar MS/MS fragmentation pattern (*m/z* 225, *m/z* 351) suggesting hydroxylation on the pyrimidine ring yielding strong correlation between *in vivo* and *in vitro* data. As such, this work also represents a practical example of a bed-to-bench approach, where a discovery from humans is then confirmed in vitro and leads to additional bench work, as that here described in this translational work.

Hydroxylation reactions of drugs are almost always catalyzed by cytochrome P450 enzymes, however, in some instances, hydroxylation of drugs containing aromatic azaheterocyclic moieties (e.g., pyrimidines and others) can be catalyzed by AO or XO. Results from experiments herein suggest that the primary biotransformation of PF-5190457 is via an NADPH-independent reaction in HLC leading to the formation of a hydroxy-pyrimidine metabolite. The position of hydroxylation on the pyrimidine ring between the two nitrogen atoms suggests nucleophilic attack via AO and/or XO enzymes in the metabolism of the drug (Krenitsky et al., 1972; Beedham, 1985; Kitamura et al., 2006). In contrast to electrophilic oxidation by CYP450 enzymes, both AO and XO enzymes catalyze their reactions by a mechanism of nucleophilic attack on carbon atoms which are electron deficient such as those adjacent to a nitrogen on aromatic N-heterocycle resulting in the formation of distinct metabolites (Krenitsky et al.,

Downloaded from dmd.aspetjournals.org at ASPET Journals on April 18, 2024

DMD Fast Forward. Published on June 10, 2019 as DOI: 10.1124/dmd.119.087015
This article has not been copyedited and formatted. The final version may differ from this version.

1972). Furthermore, the use of inhibitors indicated the contribution of both AO and XO enzymes to the formation of hydroxy pyrimidine metabolite of PF-5190457.

AO and XO enzymes belong to a family of molybdo-flavoenzymes and have a high level of similarity between their amino acid sequence (Beedham, 1987; Terao et al., 2000; Hille, 2005). The physiological relevance of AO is still not known, but XO plays an important role in catalyzing hypoxanthine to xanthine and later to uric acid (Beedham, 1985; Kitamura et al., 2006). Generally, these enzymes differ in substrate and inhibitor specificity. An increasing number of compounds in the past few decades have been identified to be substrates of these enzymes, especially involving AO which also has broader substrate specificity in comparison to XO (O'Connor et al., 2006; Pryde et al., 2010; Sanoh et al., 2015; Battelli et al., 2016). There are only a few substrates which show biotransformation by both the enzymes like 6-deoxyclovir, 6-thioxanthine, and recently VU0409106, a lead compound for childhood developmental disorders (Krenitsky et al., 1984; Morrison et al., 2012; Choughule et al., 2014). Though some overlap exists between the substrates, there have been chemical inhibitors identified specifically for AO and XO including raloxifene (Obach, 2004), hydralazine (Strelevitz et al., 2012), allopurinol (Panoutsopoulos et al., 2004) and febuxostat (Weidert et al., 2014). Allopurinol has been widely used as a known XO inhibitor, but recently it was identified that febuxostat is a more potent inhibitor of XO than allopurinol (Malik et al., 2011). There are not any important clinical drug-drug interactions associated with inhibition of AO, but as growth in new chemical entities metabolized by AO is increasing, there could arise a need to characterize the drug-drug interaction potential at the AO level (Obach, 2004; Pryde et al., 2010). Allopurinol, an XO inhibitor, significantly inhibited 6-mercaptopurine (an XO substrate) when administered orally and there was a significant increase in peak plasma concentration and area under the curve of 6-mercaptopurine in patients with acute lymphoblastic leukemia (Zimm et al., 1983). Both potent XO inhibitors, allopurinol and febuxostat, are clinically used for the treatment of chronic gout and hyperuricemia. This condition is also present in disease states like metabolic syndrome, diabetes, chronic liver disease and cardiovascular disease (Hu and Tomlinson, 2008; George and Minter, 2017). It

Downloaded from dmd.aspetjournals.org at ASPET Journals on April 18, 2024

DMD Fast Forward. Published on June 10, 2019 as DOI: 10.1124/dmd.119.087015
This article has not been copyedited and formatted. The final version may differ from this version.

is a challenge to capture the drug interactions associated with these enzymes in animal models, especially for AO, due to significant species, gender and strain-specific differences in its expression and activity (Itoh, 2009; Crouch et al., 2017; Mao et al., 2017).

The findings from this study suggest that both AO and XO contribute to the metabolism of PF-5190457 resulting in the formation of PF-6870961. In cytosol, raloxifene and febuxostat, inhibitors of AO and XO, respectively, yielded estimates of maximum inhibition values of slightly in excess of 75 and 50%, respectively. These sums to over 100% and may suggest some overlap of the inhibitor selectivity; a not uncommon phenomenon for inhibitors used in reaction phenotyping studies. The study also emphasizes the importance of these non-CYP enzymes in drug metabolism during the early stages of drug development. Preliminary in vitro work on the metabolism of this compound pre-dated findings that emerged in the literature on the potential importance of MoCo enzymes (e.g. (Magee et al., 2009; Dalvie et al., 2010; Pryde et al., 2010) and focused on the oxidative component catalyzed by cytochrome P450 enzymes. Thus, it was in human plasma samples where the first observation was made on the predominance of this metabolite ultimately found to be generated by AO and XO. This understanding of this clearance pathway for PF-5190457 will be important in its continued investigation as a therapeutic agent especially in subjects with alcohol use disorder.

In summary, this study provides important novel information from different points of view: 1) it provides additional new information on the recently developed novel compound PF-5190457, the first GHS-R1a blocker that has moved to development in humans; 2) it provides an example of a reverse translational approach where a discovery in humans was brought back, validated and further investigated at the bench level; and 3) it demonstrates the importance of considering the molybdenum-containing oxidases during the development of new drug entities.

Downloaded from dmd.aspetjournals.org at ASPET Journals on April 18, 2024

DMD Fast Forward. Published on June 10, 2019 as DOI: 10.1124/dmd.119.087015
This article has not been copyedited and formatted. The final version may differ from this version.

Acknowledgments

The authors would like to thank the research staff in the Clinical Pharmacokinetics Research Laboratory at the University of Rhode Island. The authors would also like to thank the clinical and research staff involved in data collection and support at the National Institute on Alcohol Abuse and Alcoholism (NIAAA) Division of Intramural Clinical and Biological Research, i.e., in the NIAAA/NIDA Section on Clinical Psychoneuroendocrinology and Neuropsychopharmacology and the NIAAA clinical intramural program. The authors would also like to thank the clinical and research staff involved in data collection and patient care at the NIH Clinical Center, i.e. in the Department of Nursing (in particular the nurses of the 1SE Inpatient Unit and of the 1-HALC 1SE Outpatient Clinic), in the Department of Nutrition and in the Department of Pharmacy. Furthermore, the authors would like to express their gratitude to the participants who took part in the Phase 1b clinical study. Finally, the authors would like to thank the Steering Committee of the UH2/UH3-TR000963 grant (PIs: Drs. Lorenzo Leggio and Fatemeh Akhlaghi) whose members included members from the NIAAA Division of Medication Development (in particular Dr. Joanne Fertig), the Drug Development Partnership Programs of the National Center for Advancing Translational Sciences (NCATS) and Pfizer, which kindly provided the study drug for the Phase 1b clinical study under the NCATS grant UH2/UH3-TR000963. Pfizer did not have any role in the study design, execution or interpretation of the results, and this publication does not necessarily represent the official views of Pfizer.

Conflict of interest statement

R. Scott Obach and Tim F. Ryder are active employees at Pfizer Inc., Groton, CT. All the authors have no conflict of interest to declare.

Downloaded from dmd.aspetjournals.org at ASPET Journals on April 18, 2024

DMD Fast Forward. Published on June 10, 2019 as DOI: 10.1124/dmd.119.087015
This article has not been copyedited and formatted. The final version may differ from this version.

Authorship contributions

Participated in research design: Obach, Leggio, Akhlaghi

Conducted experiments: Adusumalli, Jamwal, Obach, Ryder

Contributed new reagents or analytic tools: Obach, Leggio, Akhlaghi

Performed data analysis: Adusumalli, Jamwal, Obach, Ryder, Leggio, Akhlaghi

Wrote or contributed to the writing of the manuscript: Adusumalli, Jamwal, Obach, Ryder, Leggio, Akhlaghi

Downloaded from dmd.aspetjournals.org at ASPET Journals on April 18, 2024

DMD Fast Forward. Published on June 10, 2019 as DOI: 10.1124/dmd.119.087015
This article has not been copyedited and formatted. The final version may differ from this version.

References

Asakawa A, Inui A, Kaga T, Yuzuriha H, Nagata T, Ueno N, Makino S, Fujimiya M, Niijima A, Fujino MA, and Kasuga M (2001) Ghrelin is an appetite-stimulatory signal from stomach with structural resemblance to motilin. *Gastroenterology* **120:**337-345.

Battelli MG, Polito L, Bortolotti M, and Bolognesi A (2016) Xanthine Oxidoreductase in Drug Metabolism: Beyond a Role as a Detoxifying Enzyme. *Curr Med Chem* **23:**4027-4036.

Beedham C (1985) Molybdenum hydroxylases as drug-metabolizing enzymes. *Drug Metab Rev* **16:**119-156.

Beedham C (1987) Molybdenum hydroxylases: biological distribution and substrate-inhibitor specificity. *Prog Med Chem* **24:**85-127.

Bhattacharya SK, Andrews K, Beveridge R, Cameron KO, Chen C, Dunn M, Fernando D, Gao H, Hepworth D, Jackson VM, Khot V, Kong J, Kosa RE, Lapham K, Loria PM, Londregan AT, McClure KF, Orr ST, Patel J, Rose C, Saenz J, Stock IA, Storer G, VanVolkenburg M, Vrieze D, Wang G, Xiao J, and Zhang Y (2014) Discovery of PF-5190457, a Potent, Selective, and Orally Bioavailable Ghrelin Receptor Inverse Agonist Clinical Candidate. *ACS Med Chem Lett* **5:**474-479.

Choughule KV, Barnaba C, Joswig-Jones CA, and Jones JP (2014) In vitro oxidative metabolism of 6-mercaptopurine in human liver: insights into the role of the molybdoflavoenzymes aldehyde oxidase, xanthine oxidase, and xanthine dehydrogenase. *Drug Metab Dispos* **42:**1334-1340.

Crouch RD, Blobaum AL, Felts AS, Conn PJ, and Lindsley CW (2017) Species-Specific Involvement of Aldehyde Oxidase and Xanthine Oxidase in the Metabolism of the Pyrimidine-Containing mGlu5-Negative Allosteric Modulator VU0424238 (Auglurant). *Drug Metab Dispos* **45:**1245-1259.

Dalvie D, Zhang C, Chen W, Smolarek T, Obach RS, and Loi CM (2010) Cross-species comparison of the metabolism and excretion of zoniporide: contribution of aldehyde oxidase to interspecies differences. *Drug Metab Dispos* **38:**641-654.

Damian M, Marie J, Leyris JP, Fehrentz JA, Verdie P, Martinez J, Baneres JL, and Mary S (2012) High constitutive activity is an intrinsic feature of ghrelin receptor protein: a study with a functional monomeric GHS-R1a receptor reconstituted in lipid discs. *J Biol Chem* **287:**3630-3641.

Denney WS, Sonnenberg GE, Carvajal-Gonzalez S, Tuthill T, and Jackson VM (2017) Pharmacokinetics and pharmacodynamics of PF-05190457: The first oral ghrelin receptor inverse agonist to be profiled in healthy subjects. *Br J Clin Pharmacol* **83:**326-338.

Farokhnia M, Grodin EN, Lee MR, Oot EN, Blackburn AN, Stangl BL, Schwandt ML, Farinelli LA, Momenan R, Ramchandani VA, and Leggio L (2018) Exogenous ghrelin administration increases alcohol self-administration and modulates brain functional activity in heavy-drinking alcohol-dependent individuals. *Mol Psychiatry* **23:**2029-2038.

Fu C, Di L, Han X, Soderstrom C, Snyder M, Troutman MD, Obach RS, and Zhang H (2013) Aldehyde oxidase 1 (AOX1) in human liver cytosols: quantitative characterization of AOX1 expression level and activity relationship. *Drug Metab Dispos* **41:**1797-1804.

George C and Minter DA (2017) Hyperuricemia, in: *StatPearls*, Treasure Island (FL).

Hille R (2005) Molybdenum-containing hydroxylases. *Arch Biochem Biophys* **433:**107-116.

Howard AD, Feighner SD, Cully DF, Arena JP, Liberator PA, Rosenblum CI, Hamelin M, Hreniuk DL, Palyha OC, Anderson J, Paress PS, Diaz C, Chou M, Liu KK, McKee KK, Pong SS, Chaung LY, Elbrecht A, Dashkevicz M, Heavens R, Rigby M, Sirinathsinghji DJ, Dean DC, Melillo DG, Patchett AA, Nargund R, Griffin PR, DeMartino JA, Gupta SK, Schaeffer JM, Smith RG, and Van der Ploeg LH (1996) A receptor in pituitary and hypothalamus that functions in growth hormone release. *Science* **273:**974-977.

Downloaded from dmd.aspetjournals.org at ASPET Journals on April 18, 2024

DMD Fast Forward. Published on June 10, 2019 as DOI: 10.1124/dmd.119.087015
This article has not been copyedited and formatted. The final version may differ from this version.

Hu M and Tomlinson B (2008) Febuxostat in the management of hyperuricemia and chronic gout: a review. *Ther Clin Risk Manag* **4:**1209-1220.

Inui A, Asakawa A, Bowers CY, Mantovani G, Laviano A, Meguid MM, and Fujimiya M (2004) Ghrelin, appetite, and gastric motility: the emerging role of the stomach as an endocrine organ. *FASEB J* **18:**439-456.

Itoh K (2009) [Individual and strain differences of aldehyde oxidase in the rat]. *Yakugaku Zasshi* **129:**1487-1493.

Jamwal R, Barlock BJ, Adusumalli S, Ogasawara K, Simons BL, and Akhlaghi F (2017) Multiplex and Label-Free Relative Quantification Approach for Studying Protein Abundance of Drug Metabolizing Enzymes in Human Liver Microsomes Using SWATH-MS. *J Proteome Res*.

Kitamura S, Sugihara K, and Ohta S (2006) Drug-metabolizing ability of molybdenum hydroxylases. *Drug Metab Pharmacokinet* **21:**83-98.

Kojima M, Hosoda H, Date Y, Nakazato M, Matsuo H, and Kangawa K (1999) Ghrelin is a growth-hormone-releasing acylated peptide from stomach. *Nature* **402:**656-660.

Krenitsky TA, Hall WW, de Miranda P, Beauchamp LM, Schaeffer HJ, and Whiteman PD (1984) 6-Deoxyacyclovir: a xanthine oxidase-activated prodrug of acyclovir. *Proc Natl Acad Sci U S A* **81:**3209-3213.

Krenitsky TA, Neil SM, Elion GB, and Hitchings GH (1972) A comparison of the specificities of xanthine oxidase and aldehyde oxidase. *Arch Biochem Biophys* **150:**585-599.

Kumar GN and Surapaneni S (2001) Role of drug metabolism in drug discovery and development. *Med Res Rev* **21:**397-411.

Lee MR, Tapocik JD, Ghareeb M, Schwandt ML, Dias AA, Le AN, Cobbina E, Farinelli LA, Bouhlal S, Farokhnia M, Heilig M, Akhlaghi F, and Leggio L (2018) The novel ghrelin receptor inverse agonist PF-5190457 administered with alcohol: preclinical safety experiments and a phase 1b human laboratory study. *Mol Psychiatry*.

Leggio L (2010) Role of the ghrelin system in alcoholism: Acting on the growth hormone secretagogue receptor to treat alcohol-related diseases. *Drug News Perspect* **23:**157-166.

Leggio L, Addolorato G, Cippitelli A, Jerlhag E, Kampov-Polevoy AB, and Swift RM (2011) Role of feeding-related pathways in alcohol dependence: A focus on sweet preference, NPY, and ghrelin. *Alcohol Clin Exp Res* **35:**194-202.

Leggio L, Zywiak WH, Fricchione SR, Edwards SM, de la Monte SM, Swift RM, and Kenna GA (2014) Intravenous ghrelin administration increases alcohol craving in alcohol-dependent heavy drinkers: a preliminary investigation. *Biol Psychiatry* **76:**734-741.

Lin JH and Lu AY (1997) Role of pharmacokinetics and metabolism in drug discovery and development. *Pharmacol Rev* **49:**403-449.

Magee TV, Ripp SL, Li B, Buzon RA, Chupak L, Dougherty TJ, Finegan SM, Girard D, Hagen AE, Falcone MJ, Farley KA, Granskog K, Hardink JR, Huband MD, Kamicker BJ, Kaneko T, Knickerbocker MJ, Liras JL, Marra A, Medina I, Nguyen TT, Noe MC, Obach RS, O'Donnell JP, Penzien JB, Reilly UD, Schafer JR, Shen Y, Stone GG, Strelevitz TJ, Sun J, Tait-Kamradt A, Vaz AD, Whipple DA, Widlicka DW, Wishka DG, Wolkowski JP, and Flanagan ME (2009) Discovery of azetidinyl ketolides for the treatment of susceptible and multidrug resistant community-acquired respiratory tract infections. *J Med Chem* **52:**7446-7457.

Malik UZ, Hundley NJ, Romero G, Radi R, Freeman BA, Tarpey MM, and Kelley EE (2011) Febuxostat inhibition of endothelial-bound XO: implications for targeting vascular ROS production. *Free Radic Biol Med* **51:**179-184.

Downloaded from dmd.aspetjournals.org at ASPET Journals on April 18, 2024

DMD Fast Forward. Published on June 10, 2019 as DOI: 10.1124/dmd.119.087015
This article has not been copyedited and formatted. The final version may differ from this version.

Mao Z, Wu Y, Li Q, Wang X, Liu Y, and Di X (2017) Aldehyde oxidase-dependent species difference in hepatic metabolism of fasudil to hydroxyfasudil. *Xenobiotica*:1-8.

Morris LS, Voon V, and Leggio L (2018) Stress, Motivation, and the Gut-Brain Axis: A Focus on the Ghrelin System and Alcohol Use Disorder. *Alcohol Clin Exp Res*.

Morrison RD, Blobaum AL, Byers FW, Santomango TS, Bridges TM, Stec D, Brewer KA, Sanchez-Ponce R, Corlew MM, Rush R, Felts AS, Manka J, Bates BS, Venable DF, Rodriguez AL, Jones CK, Niswender CM, Conn PJ, Lindsley CW, Emmitte KA, and Daniels JS (2012) The role of aldehyde oxidase and xanthine oxidase in the biotransformation of a novel negative allosteric modulator of metabotropic glutamate receptor subtype 5. *Drug Metab Dispos* **40:**1834-1845.

Nagaya N, Itoh T, Murakami S, Oya H, Uematsu M, Miyatake K, and Kangawa K (2005) Treatment of cachexia with ghrelin in patients with COPD. *Chest* **128:**1187-1193.

Nagaya N, Moriya J, Yasumura Y, Uematsu M, Ono F, Shimizu W, Ueno K, Kitakaze M, Miyatake K, and Kangawa K (2004) Effects of ghrelin administration on left ventricular function, exercise capacity, and muscle wasting in patients with chronic heart failure. *Circulation* **110:**3674-3679.

Neary NM, Small CJ, Wren AM, Lee JL, Druce MR, Palmieri C, Frost GS, Ghatei MA, Coombes RC, and Bloom SR (2004) Ghrelin increases energy intake in cancer patients with impaired appetite: acute, randomized, placebo-controlled trial. *J Clin Endocrinol Metab* **89:**2832-2836.

O'Connor D, Jones P, Chambers MS, Maxey R, Szekeres HJ, Szeto N, Scott-Stevens P, Macleod AM, Braun M, and Cato B (2006) Aldehyde oxidase and its contribution to the metabolism of a structurally novel, functionally selective GABAA alpha5-subtype inverse agonist. *Xenobiotica* **36:**315-330.

Obach RS (2004) Potent inhibition of human liver aldehyde oxidase by raloxifene. *Drug Metab Dispos* **32:**89-97.

Ortiz de Montellano PR and Mathews JM (1981) Autocatalytic alkylation of the cytochrome P-450 prosthetic haem group by 1-aminobenzotriazole. Isolation of an NN-bridged benzyne-protoporphyrin IX adduct. *Biochem J* **195:**761-764.

Panoutsopoulos GI, Kouretas D, and Beedham C (2004) Contribution of aldehyde oxidase, xanthine oxidase, and aldehyde dehydrogenase on the oxidation of aromatic aldehydes. *Chem Res Toxicol* **17:**1368-1376.

Pryde DC, Dalvie D, Hu Q, Jones P, Obach RS, and Tran TD (2010) Aldehyde oxidase: an enzyme of emerging importance in drug discovery. *J Med Chem* **53:**8441-8460.

Sanoh S, Tayama Y, Sugihara K, Kitamura S, and Ohta S (2015) Significance of aldehyde oxidase during drug development: Effects on drug metabolism, pharmacokinetics, toxicity, and efficacy. *Drug Metab Pharmacokinet* **30:**52-63.

Strelevitz TJ, Orozco CC, and Obach RS (2012) Hydralazine as a selective probe inactivator of aldehyde oxidase in human hepatocytes: estimation of the contribution of aldehyde oxidase to metabolic clearance. *Drug Metab Dispos* **40:**1441-1448.

Terao M, Kurosaki M, Saltini G, Demontis S, Marini M, Salmona M, and Garattini E (2000) Cloning of the cDNAs coding for two novel molybdo-flavoproteins showing high similarity with aldehyde oxidase and xanthine oxidoreductase. *J Biol Chem* **275:**30690-30700.

Tong J, Prigeon RL, Davis HW, Bidlingmaier M, Kahn SE, Cummings DE, Tschop MH, and D'Alessio D (2010) Ghrelin suppresses glucose-stimulated insulin secretion and deteriorates glucose tolerance in healthy humans. *Diabetes* **59:**2145-2151.

Volkow ND, Wang GJ, Tomasi D, and Baler RD (2013) Obesity and addiction: neurobiological overlaps. *Obes Rev* **14:**2-18.

Downloaded from dmd.aspetjournals.org at ASPET Journals on April 18, 2024

DMD Fast Forward. Published on June 10, 2019 as DOI: 10.1124/dmd.119.087015
This article has not been copyedited and formatted. The final version may differ from this version.

Weidert ER, Schoenborn SO, Cantu-Medellin N, Choughule KV, Jones JP, and Kelley EE (2014) Inhibition of xanthine oxidase by the aldehyde oxidase inhibitor raloxifene: implications for identifying molybdopterin nitrite reductases. *Nitric Oxide* **37:**41-45.

Zallar LJ, Farokhnia M, Tunstall BJ, Vendruscolo LF, and Leggio L (2017) The Role of the Ghrelin System in Drug Addiction. *Int Rev Neurobiol* **136:**89-119.

Zimm S, Collins JM, O'Neill D, Chabner BA, and Poplack DG (1983) Inhibition of first-pass metabolism in cancer chemotherapy: interaction of 6-mercaptopurine and allopurinol. *Clin Pharmacol Ther* **34:**810-817.

Downloaded from dmd.aspetjournals.org at ASPET Journals on April 18, 2024

Footnotes

Funding source

This work was supported by the National Center for Advancing Translational Sciences [UH2/UH3-TR000963] (PIs: Drs Lorenzo Leggio and Fatemeh Akhlaghi); and by National Insititutes of Health intramural funding [ZIA-AA000218] (*Section on Clinical Psychoneuroendocrinology and Neuropsychopharmacology*; PI: Dr. Lorenzo Leggio), jointly supported by the Division of Intramural Clinical and Biological Research of the National Institute on Alcohol Abuse and Alcoholism and the Intramural Research Program of the National Institute on Drug Abuse. The content of this article is solely the responsibility of the authors and does not necessarily represent the official views of the National Institutes of Health.

Downloaded from dmd.aspetjournals.org at ASPET Journals on April 18, 2024

DMD Fast Forward. Published on June 10, 2019 as DOI: 10.1124/dmd.119.087015
This article has not been copyedited and formatted. The final version may differ from this version.

Figure legends

Fig. 1. Metabolic profiles of pooled patient plasma samples at various sampling times [predose, early (30 and 60 min), late (1350 and 1440 min)] after administration of 100 mg PF-5190457 analyzed by HPLC-UV and HPLC-MS/MS (representative *m/z* of the detected metabolites).

Fig. 2a. Representative chromatogram of PF-6870961, the major hydroxy metabolite formation in HLC.

Fig. 2b. Full scan and product ion scan of PF-6870961, the major metabolite (529a), detected at 7:30 min in the pooled human plasma samples.

Fig. 3. HPLC-MS traces for *m/z* 529 after PF-5190457 incubation in pooled human hepatocytes. Red arrows represent PF-6870961, the major hydroxy metabolite, and blue arrows represent other metabolites.

Fig. 4. ^{1}H NMR Spectra of PF-05190547 (Top) and isolation of PF-05190547 M+16 Metabolite (Bottom)

Fig. 5. Representative kinetics for the metabolism of PF-5190457 to hydroxy metabolite PF-6870961, in recombinant aldehyde oxidase incubations.

Fig. 6. Representative kinetics for the metabolism of PF-5190457 to a hydroxy metabolite PF-6870961 in human liver cytosolic incubations.

Fig. 7. Hydroxy metabolite (PF-6870961) formation in the presence of inhibitors (% of control) at various concentrations of (a) raloxifene and (b) febuxostat with 25 µM PF-5190457 in human liver cytosolic incubations.

Downloaded from dmd.aspetjournals.org at ASPET Journals on April 18, 2024

DMD Fast Forward. Published on June 10, 2019 as DOI: 10.1124/dmd.119.087015
This article has not been copyedited and formatted. The final version may differ from this version.

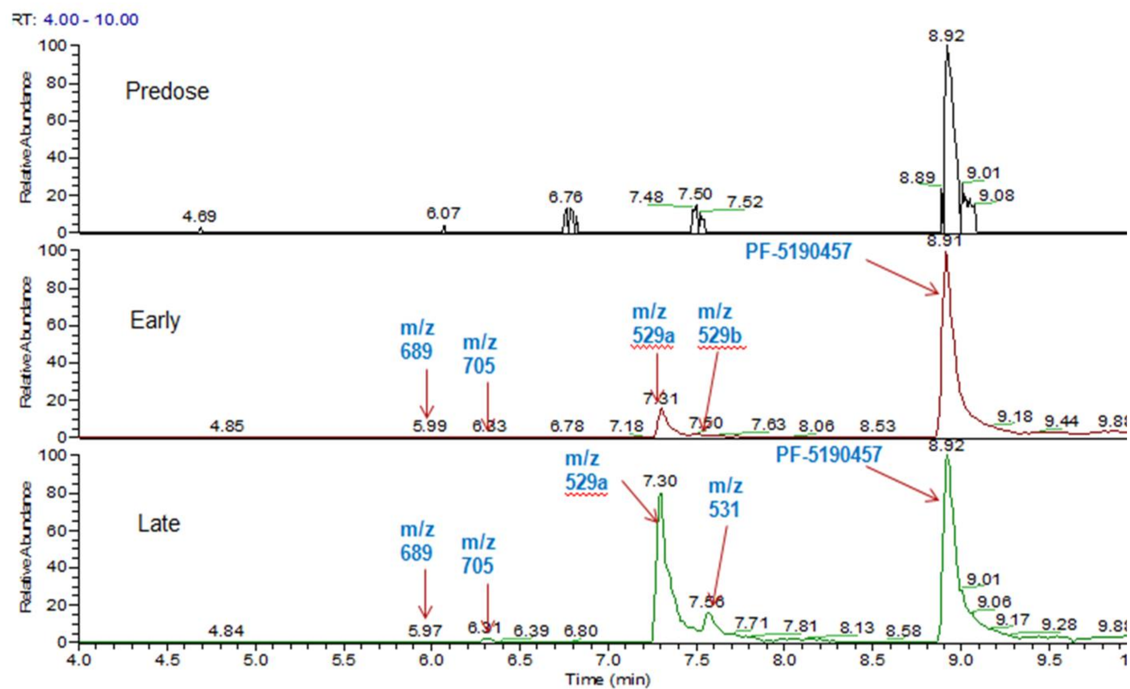

Fig. 1.

Downloaded from dmd.aspetjournals.org at ASPET Journals on April 18, 2024

DMD Fast Forward. Published on June 10, 2019 as DOI: 10.1124/dmd.119.087015
This article has not been copyedited and formatted. The final version may differ from this version.

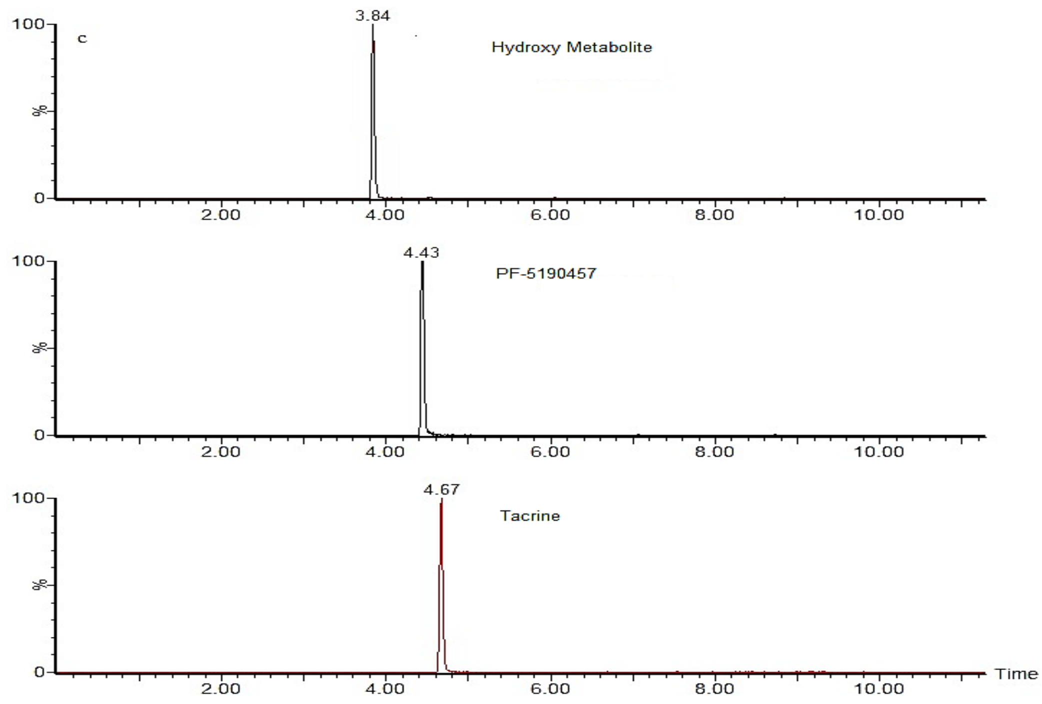

Fig. 2a.

Downloaded from dmd.aspetjournals.org at ASPET Journals on April 18, 2024

Downloaded from dmd.aspetjournals.org at ASPET Journals on April 18, 2024

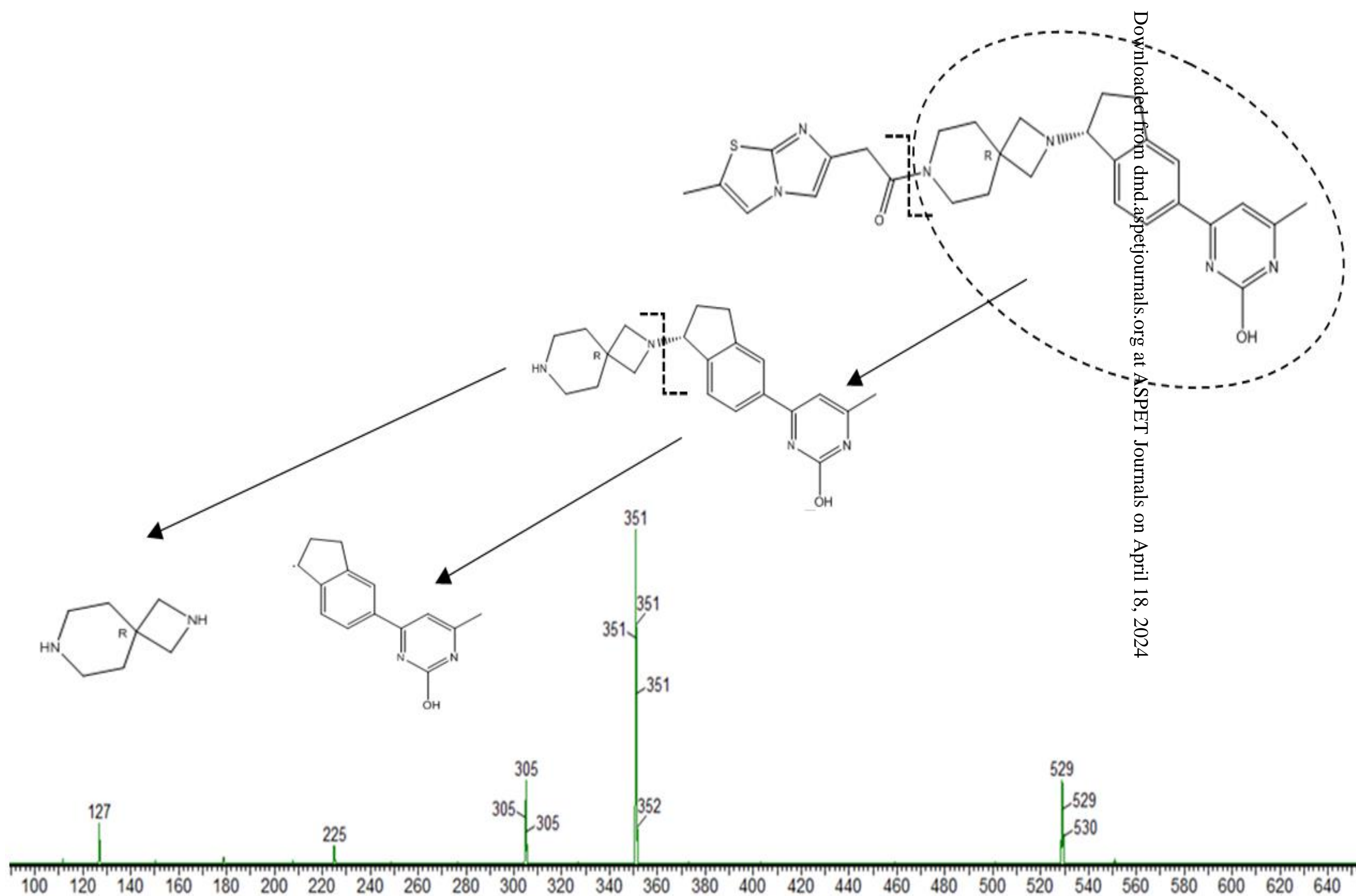

Fig. 2b.

DMD Fast Forward. Published on June 10, 2019 as DOI: 10.1124/dmd.119.087015
This article has not been copyedited and formatted. The final version may differ from this version.

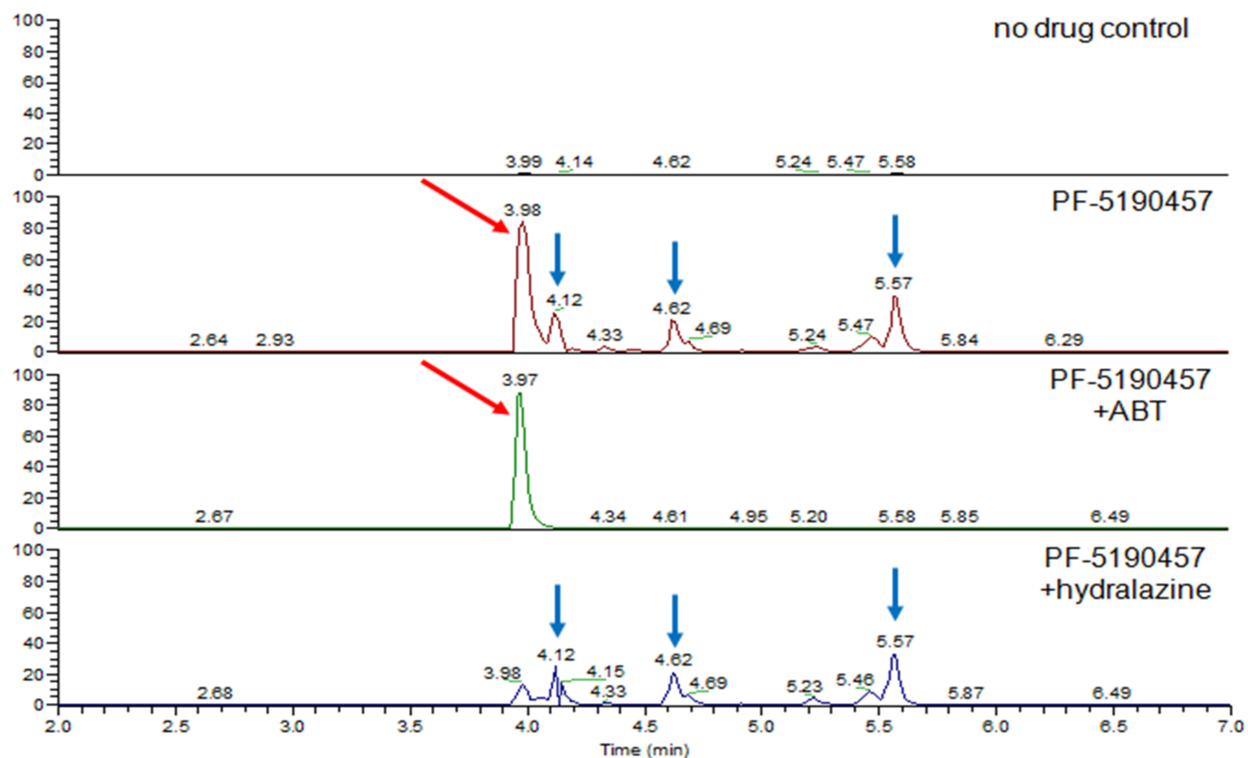

Fig. 3.

Downloaded from dmd.aspetjournals.org at ASPET Journals on April 18, 2024

DMD Fast Forward. Published on June 10, 2019 as DOI: 10.1124/dmd.119.087015
This article has not been copyedited and formatted. The final version may differ from this version.

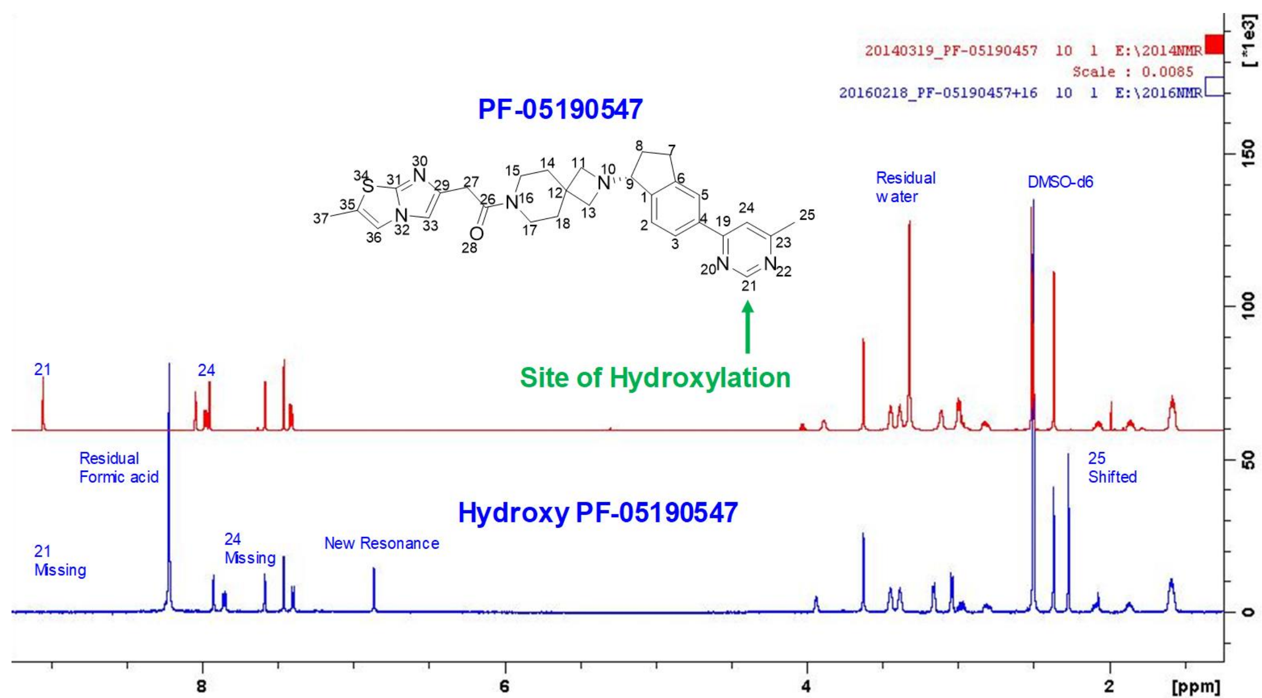

Fig. 4.

Downloaded from dmd.aspetjournals.org at ASPET Journals on April 18, 2024

DMD Fast Forward. Published on June 10, 2019 as DOI: 10.1124/dmd.119.087015
This article has not been copyedited and formatted. The final version may differ from this version.

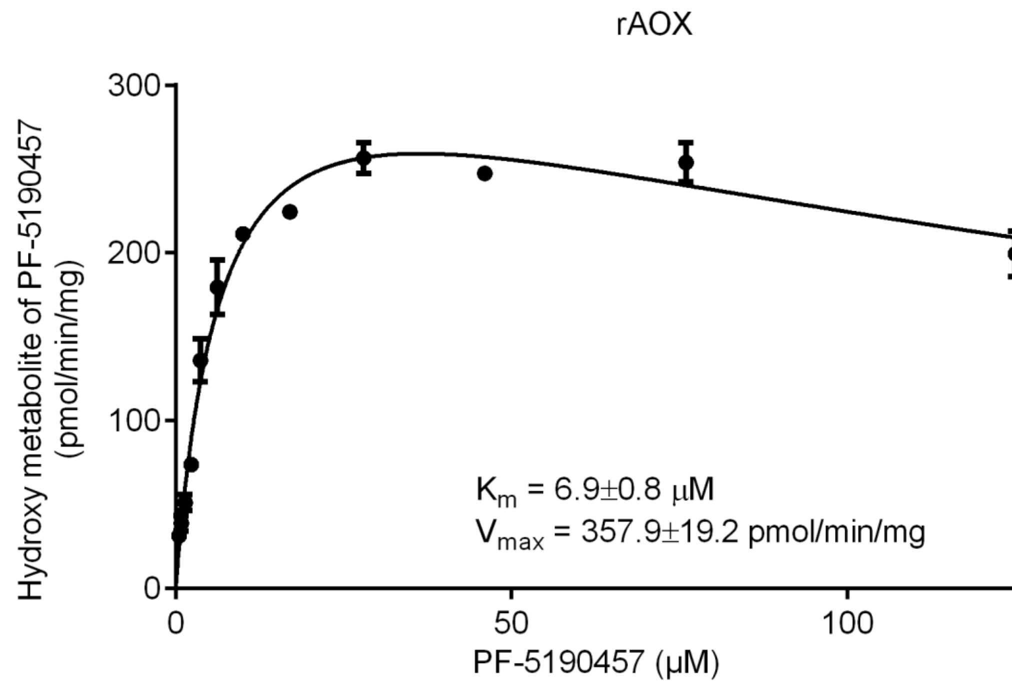

Fig. 5.

Downloaded from dmd.aspetjournals.org at ASPET Journals on April 18, 2024

DMD Fast Forward. Published on June 10, 2019 as DOI: 10.1124/dmd.119.087015
This article has not been copyedited and formatted. The final version may differ from this version.

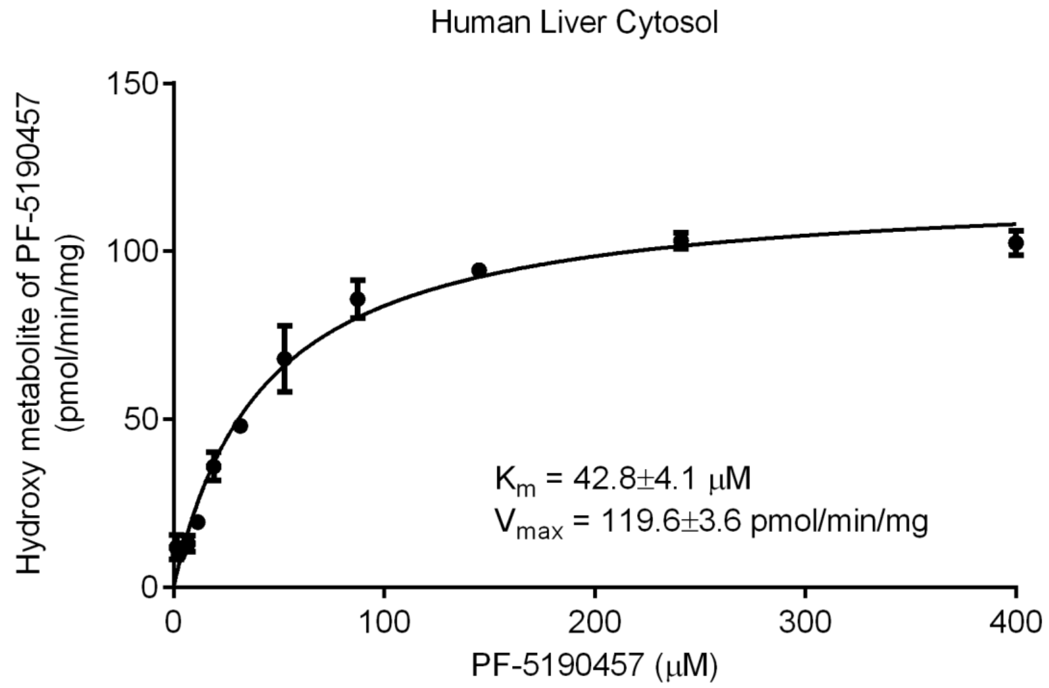

Fig. 6.

Downloaded from dmd.aspetjournals.org at ASPET Journals on April 18, 2024

DMD Fast Forward. Published on June 10, 2019 as DOI: 10.1124/dmd.119.087015
This article has not been copyedited and formatted. The final version may differ from this version.

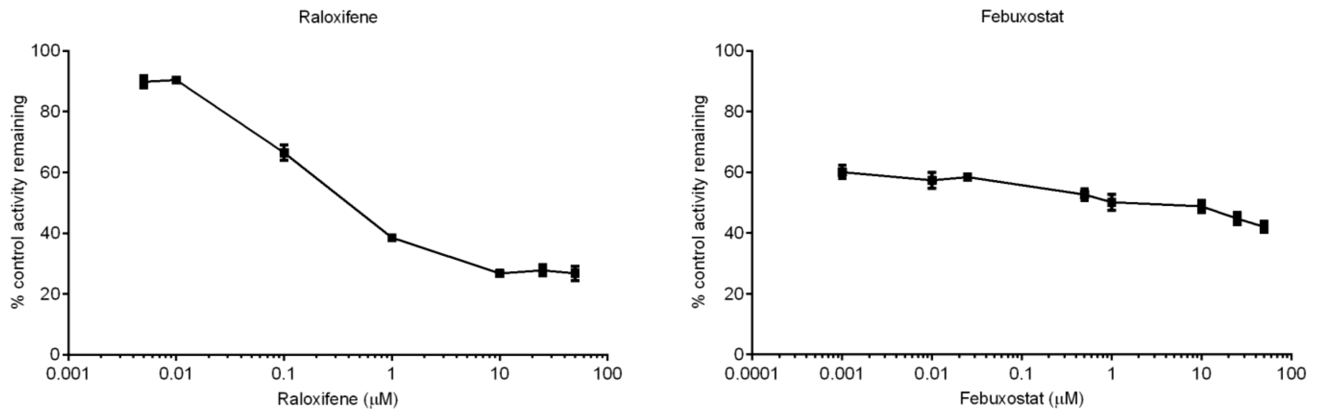

Fig. 7.

Downloaded from dmd.aspetjournals.org at ASPET Journals on April 18, 2024

DMD Fast Forward. Published on June 10, 2019 as DOI: 10.1124/dmd.119.087015
This article has not been copyedited and formatted. The final version may differ from this version.

Table 1. Mass spectrometry parameters of analytes and internal standard.

Table 1.

Compounds	Precursor (*m/z*)	Product (*m/z*)	Dwell (s)	Cone (V)	Collision energy (V)	Retention Time (min)
Parent drug (PF-5190457)	513	209, 335	0.025	30, 30	44, 16	5.6
Major hydroxyl metabolite (PF-6870961)	529	225, 351	0.025	34, 32	40, 20	4.5
Internal standard (Tacrine)	199	170, 143	0.025	46, 42	30, 36	5.9

Downloaded from dmd.aspetjournals.org at ASPET Journals on April 18, 2024